The Role of El Niño-Southern Oscillation in Regulating its Background State

De-Zheng Sun

Physical Science Division
Earth System Research Laboratory
National Oceanic and Atmospheric Administration
Boulder, Colorado

Email: Dezheng.Sun@Noaa.Gov

October 25, 2006

Abstract

A nonlinear aspect of the El Niño—Southern Oscillation (ENSO)--its regulatory effect on the background state (the climatological state)--is described. In particular, it is shown that ENSO acts as a basin-scale heat "mixer" that prevents any significant increase from occurring in the time-mean difference between the warm-pool SST (Tw) and the temperature of the thermocline water (Tc). When this temperature contrast is forced to increase, the amplitude of ENSO increases—El Niño becomes warmer and La Niña becomes colder. A stronger La Niña event results in more heat transported to the subsurface of the western Pacific. A stronger El Niño event then warms the eastern Pacific and cools the western Pacific. The effect of a stronger La Niña event does not cancel the effect from a stronger El Niño event. The long-term mean effect of ENSO—the recurrent occurrence of El Niño and La Niña events--is to mix heat downward across the equatorial Pacific and prevent the time-mean difference between Tw and Tc from exceeding a critical value.

The results have implications for several climatic issues and these implications are discussed. In particular, it is noted that our existing paradigm to understand the response of ENSO to global warming needs to be modified. It is emphasized that it is the tendency in the stability forced by increased greenhouse effect, not the actual changes in the time-mean climate, that ENSO responds to. Changes in the latter—changes in the mean

climate—are a residual between the effect of the changes in the radiative forcing and the effect of the changes in the ENSO behavior.

1. Introduction

Among our many questions about the behavior of the Earth's climate system, one stands out prominently. The question is whether natural variability in the state of the climate system-- the temporal instability in the climate system --plays a role in regulating the long-term stability of the climate system. (An adjunct question is whether natural variability plays a role in determining the sensitivity and stability of the climate system to anthropogenic forcing). In this context, the role of El Niño-Southern Oscillation (ENSO) in determining the climatological state of the coupled ocean-atmosphere system stands as a fundamental issue in the sciences of global climate change and by extension a fundamental issue in geosciences.

Although the last 20 years has witnessed heightened research activity in understanding the nature of ENSO (Neelin et al 1998, Wang et al. 2004), the nonlinear aspects of ENSO in general, its interaction with the mean background flow in particular, have just began to be revealed. This article highlights some progress we have made on this front of research with a focus on the role of ENSO in regulating the time-mean difference between the sea surface temperature of the warm-pool (Tw) and the temperature of the equatorial undercurrent (Tc). Because the water feeding the equatorial undercurrent ultimately comes from the high latitudes, and because the poleward heat transport depends on the vertical mixing of heat in the tropical oceans, we point to a possible role of ENSO in determining the equator and pole temperature differences and thereby the mean surface temperature of the planet Earth.

The article is organized as follows. We first describe some phenomenological aspects of ENSO and highlights the fact that ENSO corresponds to a zonal “sloshing” of the water in the equatorial upper Pacific (Section 2). In section 3, we briefly review the linear theories that have developed to explain the occurrence of the ENSO phenomenon. We will point out there that the linear theories, while quite successful in explaining the ENSO anomalous variability about a prescribed background state, left unaddressed the question whether ENSO in turn plays a role in determining the background state. We then proceed to discuss the background studies that have lead to the present hypothesis about the role of ENSO in regulating its background state, and we will present the results from coupled experiments that have been explicitly designed to test the hypothesis (Section 4). Finally, we discuss the implications of our results (section 5).

2. Some observed hallmarks of ENSO

Even though the incoming solar radiation at the outer boundary of the climate system is zonally symmetric over the equatorial Pacific, the equatorial western Pacific is considerably warmer than the equatorial eastern Pacific (Fig.1a). The warm water in the equatorial western Pacific—the warm water enclosed by the 20^{o}C SST contour in particular—is often referred to as the western Pacific warm-pool. The western Pacific warm-pool has the maximum sea surface temperature of the Earth’s open oceans. The western Pacific warm-pool is a fairly deep structure and therefore contains a huge amount of heat (Fig. 1b). The warm-pool region acts as a major “furnace” of the climate system because tropical deep convection is concentrated there and the resulting latent release drives the planetary-scale circulations in the atmosphere which in turn drives the circulations in the oceans (Fig.1c). The cold-SST in the equatorial eastern Pacific results from a wind-driven shoring of the thermocline in that region and the associated cold water upwelled to the surface to feed the surface divergence. The “tongue-like” shape in the SST distribution in the eastern equatorial Pacific has led to the term “equatorial Pacific cold-tongue”.

The warm-pool—cold-tongue configuration is not steady. The relative size of the warm-pool and the cold-tongue varies on a range of time-scales. The most profound change occurs on the inter-annual time-scales. Every 2—7 years, the western Pacific warm-pool extends to the east and causes anomalous warming in the central and eastern equatorial Pacific (Fig.2ab). This eastward displacement also displaces the deep convection eastward and is associated with a weakening of the normally eastward trade winds which is in turn associated with a zonal redistribution of heat in the equatorial upper ocean (Fig. 2c). This eastward displacement is called El Niño. An El Niño event is often followed by a westward extension of the cold-tongue. The resulting anomalous decrease in the eastern and central equatorial Pacific SST is called La Niña. Accompanying with this alternating extension and retreat of the warm-pool or cold-tongue are the alternating strengthening and weakening of the trade winds. This quasi-periodic eastward extension of the western Pacific warm-pool and the associated atmospheric changes are called El Niño—Southern Oscillation (ENSO). As trade winds upon the equatorial Pacific strengthens and weakens during the ENSO cycle, the upper ocean water moves back and forth zonally as well as meridionally (Neelin et al 1999)—ENSO effectively “sloshes” the water in the equatorial upper ocean, particularly in the zonal direction.

3. Explaining ENSO—the linear perspective

A milestone in our understanding of ENSO is the numerical model of Zebiak and Cane (1988). This model underscores two important elements for the recurrent occurrence of El Niño events which result in repeatedly “sloshing” of water in the equatorial upper ocean. One is the Bjerknes feedback—the positive feedback loop among anomalous SST, anomalous surface winds, and anomalous upwelling. This positive feedback loop enables an initial surface warming in the central and eastern Pacific to grow (Neelin et al. 1998).

The model of Zebiak and Cane (1988) is an anomaly model for ENSO, however. The model has the subsurface temperature fixed, and consequently had to resort to something that is empirical to wrap up the instability. This empirical fix is a prescribed relationship between the temperature of the upwelling water and the depth of the equatorial thermocline. Nonetheless, the model results suggested another element that is later proven quite relevant to the real system—the delayed negative feedback from the ocean dynamics (Schop and Suarez 1988, Battisti 1988). The nature of the delayed negative feedback is further clarified by the discharge and recharge oscillator as the latter explicitly links the negative feedback and the associated ocean dynamics to the heat transport process. Yet the theory remains a theory for an anomaly and requires the prescription a background state. The background state is usually chosen as the observed climatological state. The question whether ENSO in return affects the climatological state is unaddressed.

Another school of thought on the origin of El Niño events is the stochastic theory of ENSO (Penland and Sardeshmukh 1995). Based on linear inverse modeling of ENSO, these authors argue that ENSO can be explained by a linear system forced by noise. They further interpret the noise as a way to represent the unresolved nonlinearity or the weather events or the combination of the two. Again, this view requires a prescription of a fixed background state, leaving the question whether ENSO in turn plays a role in determining the background state unaddressed.

4. The effects of ENSO on its background state

4.1 Some background material

The theoretical study of Sun and Liu (1996) first suggested the importance of the basin-scale coupling between the atmosphere and ocean in regulating the tropical maximum SST and by the extension the importance of the basin-scale coupling in regulating the time-mean tropical Pacific climate. Since ENSO results from the same basin-scale coupling between the atmosphere and ocean, the study of Sun and Liu (1996) heightened the interest in the role of ENSO in the long-term heat balance of the tropical Pacific. Subsequent analysis of the observed heat balance in the tropical Pacific reveals that ENSO is fundamentally involved in the heat transport in the tropical Pacific (Sun and Trenberth 1997, Sun 2000). Sun and Trenberth (1997) noted that during the 1986-87 El Niño event, there is not only marked increase in cloud reflection of solar radiation, but also marked increase in the pole-ward heat transport in the atmosphere and ocean. The extended study by Sun (2000) and Sun (2003) further show that transporting heat poleward away from the equatorial Pacific episodically through El Niño events is actually the norm of the way by which equatorial Pacific pushes pole-ward the heat absorbed over the equatorial Pacific Pacific. The numerical experiments by Sun (2003) and Sun et al. (2004) show that when the coupled tropical ocean-atmosphere is "demanded" to transport more heat from the equatorial Pacific to the higher latitudes through an increase in the surface heating over the tropical ocean or through an increase in the surface cooling over the subtropical ocean, ENSO becomes more energetic. This result confirms the intuitive notion that has been developed from the observational analysis that ENSO corresponds to a heat transport mechanism. The numerical experiments also help to clarify the role of La Niña, which is to pump heat downward. Not like in the tropical atmosphere where an ascending parcel can become buoyant once it is lifted above the boundary layer, and can therefore continue the ascent self-propelled, warm surface water in the tropical Pacific has to be pumped downward through strong winds which occur during the La Niña phase. The notion that ENSO acts as heat transfer mechanism is therefore raised. Sun (2004) use the word "heat-pump" to describe this emerging picture about ENSO.

4.2 The focus of the present article

If ENSO corresponds to a mechanism of downward and poleward heat transport, there is a good chance that ENSO may play a role in stabilizing the time-mean state of the coupled tropical Pacific ocean-atmosphere system. The reasoning here is similar to the reasoning that has led to the hypothesis that the neutrality of the time-mean thermal structure of the tropical troposphere to moist convection is due to moist convection (Xu and Emanuel 1989). As radiative heating of the surface and cooling of the interior of the atmosphere destabilizes the atmosphere, moist convection takes place to deliver heat from the surface to the free troposphere. Consequently, the mean lapse rate is strongly regulated. Just as there is evidence indicating that the mean lapse rate of the tropical troposphere is strongly regulated, there is also evidence indicating that the stability of the long-term mean state of the coupled tropical ocean-atmosphere system is regulated (Penland and Sardeshmukh 1995, Penland et al. 2000).

A key parameter that determines the stability of the coupled tropical ocean-atmosphere system is the difference between the warm-pool SST (Tw) and the temperature of the equatorial undercurrent (Tc) (Fig.3). This is because a larger difference between Tw and Tc would result in a stronger zonal SST contrast and thereby stronger zonal winds and stronger zonal tilt of the equatorial thermocline (Jin 1996, Sun 1997).

Increased tropical heating tends to raise Tw. Extratropical cooling tends to cool Tc as the water feeding the equatorial undercurrent comes from the extratropics (McCreary and Lu 1994, Pedlosky 1987). Our curiosity is whether the presence of ENSO reduces the sensitivity of Tw-Tc to either an increase in the tropical heating or an increase in the subtropical/extratropical cooling.

Our curiosity about the role of ENSO in determining the equatorial upper ocean thermal stratification is also driven by a hallmark of the ENSO phenomenon-- the zonal “sloshing” of water in the equatorial upper Pacific. Given this correspondence, it is of interest even from a purely phenomenological perspective to investigate the effect of the recurrent occurrence of ENSO on the time-mean upper ocean temperature structure which is characterized by the time mean difference between Tw and Tc.

In light of the results from the observations, we have the following hypothesis concerning the effects of ENSO on its background state: The recurrent occurrence of El Niño and La Niña events--ENSO--may be a mechanism that regulates the time-mean thermal stratification of the equatorial upper ocean, and more generally the stability of the long-term mean state of the coupled tropical Pacific ocean-atmosphere system.

4.3 The methodology

Our method to test this hypothesis is through conducting numerical experiments in pairs with a coupled model. In one experiment, the ENSO is turned off. We turn off ENSO in the model by setting the coupling coefficients between the SST and surface winds in the equatorial region to zero. In the other experiment, ENSO is kept on. We then contrast the differences in the response in the time-mean climate, the difference between Tw and Tc in particular as it determines the stability of the time-mean climate.

The perturbation takes the form of either increased radiative heating over the tropics or alternatively increased radiative cooling over the subtropics. For reasons mentioned in the introduction, changes like these tend to increase the difference between Tw and Tc and thereby tends to destabilize the coupled climate system.

The model is the one used in Sun (2003) and Sun et al. (2004). The model has the NCAR Pacific basin model (Gent and Cane 1989) as its ocean component. Thus the model calculates the upper ocean temperatures based on the first principles. This feature is in contrast with the intermediate ocean models used in the pioneering studies of ENSO (Neelin et al. 1998). (Intermediate ocean models do not have a heat budget for the subsurface ocean). The parameterization of the heat flux and zonal wind stress in the present model, however, are in line with those used in previous theoretical studies of ENSO and tropical climatology (Neelin et al. 1998). Specifically, we assume that the surface heat flux is proportional to the difference between the radiative convective equilibrium sea surface temperature (SSTp) and the actual SST. This parameterization is supported by observations (Sun and Trenberth 1998) and aids the changes of radiative heating in the perturbation experiments. The model simulates the observed characteristics of ENSO including the subsurface temperature evolution of the life cycle of ENSO (Sun 2003).

4.4 *Tropical heating experiments*

Table 1 shows the response in Tw, Tc, and Tw-Tc in three pairs of the perturbation experiments. The three pairs are presented here and they differ in the regions where an enhanced tropical heating is applied. In all these pairs, the response in Tw-Tc in the presence of ENSO is much reduced than in the absence of ENSO. Take pair II as an example, change in Tw-Tc in the absence of ENSO is about 1.3 ^{o}C. With ENSO this change is reduced to 0.1 ^{o}C, following a reduction in the increase in Tw and an increase in Tc. Apparently, the presence of ENSO reduces the surface warming and increase the response in the subsurface.

Fig.4a and Fig.4b provide a more detailed look of the response in the time-mean temperature in the equatorial upper ocean. These two figures show respectively the equatorial temperature differences between the control run and the perturbed run for the case with ENSO and for the case without ENSO. Without ENSO, the warming of the tropical ocean is essentially confined in the surface layer. On the right is the case with ENSO. With ENSO, the response extends to the themocline. The thermocline water is also warmer while the response at the surface level is reduced, particularly in the western Pacific. The presence of ENSO also appears to warm slightly the surface ocean of the central Pacific (180^o-240^oE) and cools the surface ocean near the eastern boundary

To understand these differences, we note that the ENSO is stronger in response to enhanced tropical heating. Fig. 5 shows the Niño3 SST time-series from the control run and the perturbed run. The figure shows that in response to the increase in the tropical heating, El Niño events become warmer while the La Niña events become colder. The variance of the Niño3 SST in the perturbed run more than doubles the variance of the Niño3 SST in the control run (the variance changes from 0.55 ^oC to 1.3 ^oC). The changes in Niño3 SST variance in the other two pairs of experiments are respectively from 0.55 ^oC to 1.35 ^oC. Clearly, ENSO in this model is sensitive to tropical heating.

Stronger La Niña enables more heat to be transported downward to the subsurface ocean, the western Part of the ocean in particular in the equatorial region. The left panel on Fig. 6 shows the upper ocean temperature changes during La Niña events in response to the enhanced tropical heating. The thermocline is deeper in the western Pacific consistent with the stronger zonal winds. The right panel on Fig. 6 shows the temperature differences in the warm-phase. Stronger El Niño events then warm the upper ocean in the central and eastern Pacific. Averaged over the cold and warm phases, the heat is “mixed” downward across the basin. Note the asymmetry between changes in the upper ocean temperature during the La Niña phase (Fig.6a) and the El Niño phase (Fig.6b).

4.5: Extratropical cooling experiments:

An important finding of the last decade or so in physical oceanography is that the equatorial thermocline water originates from the extratropical surface ocean. Surface water in the subtropical/extratropical ocean is pumped downward and equatorial ward and eventually feed the equatorial undercurrent and the equatorial upwelling water (McCreary and Lu 1994, Pedlosky 1987). This tropical extratropical/subtropical connection has been referred to as the “ocean tunnel” and is schematically shown in Fig. 7. If you cool the extratropical/subtropical surface ocean, you can cool the equatorial thermocline water and thereby destabilize the coupled system over the equatorial Pacific. But again, we will see that the response in the temperature of the equatorial undercurrent (Tc) to a cooling imposed over the subtropical/extratropical ocean depends critically on whether the system has ENSO or not.

Table 2 shows the response in Tw, Tc and Tw-Tc in three pairs of the perturbation experiments. The three pairs are presented here and they differ in the regions where an enhanced subtropical/extratropical cooling is applied. In all these pairs, the response in Tw-Tc in the presence of ENSO is much reduced than in the absence of ENSO. In fact, the value of Tw-Tc in the perturbed cases is even slightly smaller than in the corresponding control case. Take pair II as an example, change in Tw-Tc in the absence of ENSO is about 0.53 ^{o}C. With ENSO this change is -0.22 ^{o}C, following an increase in the cooling Tw and a reduction in the cooling to Tc. Apparently, the presence of ENSO reduces the subsurface cooling and increases the cooling the surface ocean in the western Pacific.

Fig.8a and Fig.8b provide a more detailed look of the response in the time-mean temperature in the equatorial upper ocean. These two figures show respectively the equatorial temperature differences between the control run and the perturbed run for the case with ENSO and for the case without ENSO. Without ENSO, the equatorial thermocline water is cooled by about 1 ^{o}C by the imposed cooling over the extratropical surface ocean. With the presence of ENSO, the cooling to the equatorial thermocline water is reduced to about 0.5 ^{o}C.

To understand these differences, we note again that the ENSO is stronger in response to enhanced extratropical cooling. Fig. 9 shows the Niño3 SST time-series from the control run and the perturbed run. The El Niño events become warmer while the La Niña events become colder. Just as in the enhanced tropical heating case, stronger La Niña enables more heat to be transported downward to the subsurface ocean, the western Part of the ocean in particular in the equatorial region. The left panel on Fig. 10 shows the upper ocean temperature changes during La Niña events in response to the enhanced tropical heating. The thermocline water in the western Pacific is actually warmer despite the imposed cooling. The right panel on Fig. 10 shows the temperature differences in the warm-phase. Stronger El Niño events then warm the upper ocean in the central and eastern Pacific. Averaged over the cold and warm phases, the cooling to the equatorial thermocline water is significantly reduced.

Fig. 11 further shows a meridional section of the ocean temperature change at the central Pacific. Again, the left is the case without ENSO, and the right panel is for the case with ENSO. The "tunneling" effect is very obvious in the case without ENSO. In the presence of ENSO, the temperature anomalies in the equatorial region are so much reduced that the equatorial region appears to be disconnected from the higher latitudes. This may provide an explanation for why studies using observational data tend to show that decadal temperature anomalies originates from the extratropical surface Pacific largely disappear once they reach near equatorial region (Schneider et al. 1999). The real world has ENSO which effectively destroys the decadal signals originating from the extratropics though effective mixing in the tropical Pacific. Therefore the apparent disappearance of decadal temperature anomalies upon their reach to the equatorial region in the observations does not suggest an ineffective extratropical influence over the level of ENSO activity.

5. **Summary and Conclusion**

A fundamental question about the Earth's climate system is whether natural variability in the state of the climate system-- the temporal instability in the climate system --plays a role in regulating the long-term stability of the climate system. To shed light on this question, we have carried out numerical experiments to investigate the role of ENSO in regulating the stability of the time-mean state of coupled tropical Pacific ocean-atmosphere system. The results suggest that ENSO acts a basin-scale heat mixer that prevents any significant increase from occurring in the time-mean differences between the warm-pool SST (Tw) and the temperature of the thermocline water (Tc).). Because the water feeding the equatorial undercurrent ultimately comes from the high latitudes, and because the poleward heat transport depends on the vertical mixing of heat in the tropical oceans, we point to a potential role of ENSO in determining the equator and pole temperature differences and thereby the mean surface temperature of the planet Earth.

The finding that ENSO regulates the climatological difference between Tw and Tc has several implications. First, given the efficiency ENSO in removing heat from the surface ocean to the subsurface ocean, one naturally wonder about the reliability of prediction of global warming made by climate models that do not have good simulations of ENSO. Without adequate ENSO in the models, the heat uptake of the equatorial upper oceans and the poleward heat transport by the oceans may be underestimated by the models. This prediction may be tested with the output of coupled models.

The results also imply that some biases in the mean climate simulated by the coupled climate models in the tropical Pacific, such as the excessive cold-tongue (Sun et al. 2006), may not just be an cause for errors in the simulated ENSO—it could well be a consequence of the poor simulation of ENSO. The cold-bias in the SST over the central and eastern equatorial Pacific in the coupled models may be indicative of a colder equatorial undercurrent due to an insufficient downward heat mixing by ENSO. This is clearly a conjecture at this stage, but can be tested with the outputs from the coupled models—through analyzing ENSO and the subsurface temperatures of the coupled models. In the same vein, the present finding suggests that the tropical Pacific decadal variability may be more a consequence of the decadal variations in the level of ENSO activity than a cause of them. Therefore, the present results echo the concern raised by Schopf and Burgman (2005). The results also lend support to the suggestion by Rodger et al (2004) and Yeh and Kirtman (2004).

Finally, the present finding suggests a need to revise the paradigm that we have used to understand how ENSO may respond to global warming. The traditional paradigm used in understanding the impact of anthropogenic forcing on ENSO is schematically shown in the upper panel of Fig. 12. The procedure is that one first finds out the impact of an increase in CO2 on the mean climate—the climatological state, then use the realized changes in the climatological state to deduce the response of ENSO. (For a recent study that epitomizes this procedure, see Fedorov and Philander (2000)). The underlying assumption in this procedure is that changes in ENSO are a passive response to changes in the time-mean climate --ENSO is not involved in determining the changes in the background state. The present finding suggests, however, that ENSO is fundamentally involved in determining at least certain aspects of its background state or the time-mean climate. In particular, the present findings suggest that it is the tendency in the stability forced by increased greenhouse effect, not the actual changes in the time-mean climate, that ENSO responds to. Changes in the latter—changes in the mean climate—are a residual between the effect of the changes in the radiative forcing and the effect of the changes in the ENSO behavior. Indeed, in a recent statistical analysis by Tsonis et al. (2005), it is found that changes in ENSO statistics are correlated with the tendencies in the global mean surface air temperature, but not with the global mean surface air temperature itself. Accumulating evidence suggest that it may be high time for us to modify our paradigm-- ENSO needs to be considered at least a significant feedback mechanism in our effort to figure out the consequences of anthropogenic forcing on ENSO and on the climatological state. This revised paradigm is schematically shown in the lower panel of Fig. 12.

References:

Battisti, D.S., 1988: The dynamics and thermodynamics of a warm event in a coupled ocean-atmosphere model, *J. Atmos. Sci,* ***45,*** 2889-2919**.**

Carton, J.A., G. Chepurin, X. Cao, and B.S. Giese, 2000a: A Simple Ocean Data Assimilation analysis of the global upper ocean 1950-1995, Part 1: methodology, *J. Phys. Oceanogr*., **30**, 294-309.

Fedorov, A.V., and S.G. Philander, 2000: Is El Nino Changing? *Science*, **288**, 1997—2002.

Gent, P.R., and M.A. Cane, 1989: A reduced gravity, primitive equation model of the upper equatorial ocean. *J. Compute. Phys*., **81**, 444-480.

Jin, F.F., 1996: Tropical ocean-atmosphere interaction, the Pacific cold-tongue, and the El Nino-Southern Oscillation. *Science*, **274**, 76-78.

Kalnay, E. and 21 coauthors, 1996: The NCEP/NCAR 40-year reanalysis project. *Bull. Amer. Meteor. Soc.*, **77**, 437-471.

Neelin, J.D., D.S. Battiti, A.C. Hirst, F.F. Jin, Y. Wakata, T. Yamagata, and S. Zebiak, 1998: ENSO Theory. *J. Geophys. Res*., **103**, 14261—14290.

Penland, C., Flügel, M., and P. Chang, 2000: Identification of Dynamical Regimes in an Intermediate Coupled Ocean-Atmosphere Model. *J. of Climate*, **13**, pp.2105-2115.

Penland, C, and PD Sardeshmukh, 1995: The Optimal Growth of Tropical Sea Surface Temperature Anomalies. *J. Climate,* **8**, 1999-2024.

Philander, S.G., 1990: El Nino, La Nina, and the Southern Oscillation. Academic Press, New York, 293 pp.

Rodgers, K.B., P. Friederichs, and M. Latif, 2004: Tropical Pacific Decadal Variability and its Relation to Decadal Modulations of ENSO. *J. Climate,* **17**, 3761—3774.

Schopf, P. and R. Burgman, 2005: A Simple Mechanism for ENSO Residuals and Asymmetry. *J. Climate*, Accepted.

Schneider, N., A. J. Miller, M.A. Alexander, C. Deser, 1999: Subduction of Decadal North Pacific Temperature Anomalies: Observations and Dynamics, *J. Phys. Oceanogr.,* **29**, 1056-1070.

Shin, S.-I and Z. Liu, 2000: Response of the equatorial thermocline to extratropical buoyancy forcing. *J. Phys. Oceanogr.*, **30**, 2883-2905.

Sun, D.-Z., 1997: El Niño: a coupled response to radiative heating? *Geophys. Res. Lett.*, **24**, 2031-2034.

Sun, D.-Z., 2000: The heat sources and sinks of the 1986-87 El Niño, *J. Climate*, **13**, 3533-3550.

Sun, D.-Z., 2003: A Possible Effect of An Increase in the Warm-pool SST on the Magnitude of El Niño Warming. *J. Climate*, **16**, 185-205.

Sun, D.-Z. and Z. Liu, 1996 : Dynamic ocean-atmosphere coupling: a thermostat for the tropics. *Science*, **272**, 1148-1150.

Sun, D.-Z. and K.E. Trenberth, 1998: Coordinated heat removal from the equatorial Pacific during the 1986-87 El Niño. *Geophys. Res. Lett.*, **25**, 2659-2662.

Sun, D.-Z., T. Zhang, C. Covey, S. Klein, W.D. Collins, J.J. Hack, J.T. Kiehl, G.A. Meehl, I.M. Held, and M. Suarez, 2005: Radiative and Dynamical Feedbacks Over the Equatorial Cold-tongue: Results from Nine Atmospheric GCMs. *J. Climate* , **19** , 4059-4074.

Sun, D.-Z., T. Zhang, and S.-I. Shin, 2004 : The effect of subtropical cooling on the amplitude of ENSO: a numerical study. *J. Climate,* **17**, 3786-3798.

Wang, C., S.-P. Xie, and J. A. Carton, 2004: A global survey of ocean-atmosphere interaction and climate variability. In: *Earth's Climate: The Ocean-Atmosphere Interaction.* C. Wang, S.-P. Xie, and J. A. Carton, Eds., AGU Geophysical Monograph.

Tsonis, A.A. ,J.B. Elsner, A.G. Hunt and T.H. Jagger, 2005: Unfolding the relation between global temperature and ENSO*. Geophys. Res. Lett.* doi:10.1029/2005GL022875 .

Xie, P., and P.A. Arkin, 1996: Analyses of Global Monthly Precipitation Using Gauge Observations, Satellite Estimates, and Numerical Model Predictions. *J. Climate,* 9, 840-858.

Xu, K.M., and K. Emanuel, 1989: Is the tropical atmosphere conditionally unstable? Mon. Wea. Rev., 117, 1471-1479.

Yeh, S.-W. and B.P. Kirtman, 2004: Tropical decadal variability and ENSO amplitude modulations in a CGCM*. J. Geophys. Res.,* **109**, doi:10.1029/2004JC002442.

Acknowledgement

The research was supported by NOAA and NSF (ATM-9912434, ATM-0332760, and ATM 0553111).

Table Legends:

Table 1: Response of Tw, Tc, and Tw-Tc to an enhanced tropical heating with and without ENSO. The definitions of Tw and Tc are the same as in Sun et al. (2004). The three pairs presented here differ in the meridional extent of the regions where an enhanced tropical heating is applied. Anomalous heating is confined to 5^oS-5^oN for Pair I, 10^oS-10^oN for Pair II, and 15^oS-15^oN for Pair III. In all three cases, the increase in the radiative convective equilibrium SST (SSTp) peaks at the equator with a value of 2^oC, and then decrease with latitude following a cosine profile to zero at the specified latitudes (i.e., 5^o, 10^o, and 15^o respectively for the three cases). The last 3 years of data of a 27-year-long run are used in the calculation for the case without ENSO, and the last 23 years of a 27-year-long run are used in the calculation for the case with

Table 2: Response of Tw,Tc, and Tw-Tc to enhanced subtropical/extratropical cooling with and without ENSO. Three pairs are presented here and they differ in the regions where an enhanced subtropical heating is applied. Pair I corresponds to the case where anomalous subtropical cooling—a reduction in SSTp--starts from 5^o. Pair II corresponds to the case where anomalous subtropical cooling starts from 10^o Pair III corresponds to the case where anomalous subtropical cooling starts from 15^o. In all three cases, the reduction in SSTp increases monotonically with latitude to a fixed value 1^oC at $30^oS(N)$. The last 3-year average of a 27-yr-long run are used in the calculation for the case without ENSO. For the three cases with ENSO, the last 23 year of a 36 year long run is used for the case in Pair I, the last 23 years of a 40 year run was used for the case in pair II, and the last 23 years of 56 year long run are used in the calculation for the case in pair

III. As the cooling is moved progressively to a higher latitude, there is more delay for the onset of the region with stronger ENSO and consequently there is a need for a longer run to obtain a time series of Niño3 SST that is representative of the regime.

Figure Legends

Fig.1: (a) Climatological global SST distribution. The arrows in green show the corresponding surface currents. (b) The corresponding equatorial upper ocean temperature distribution (5^oS-5^oN). (c) The corresponding distribution of precipitation and surface wind stress. Shown are winter conditions (Nov.-Dec.). The SST and currents data are from the global ocean analysis (Carton et al. 2000). The surface winds data are from the NCEP reanalysis (Kalnay et al. 2000). The precipitation data are from Xie and Arkin (1996).

Fig.2: (a) Global SST distribution for the 1982-83 winter. The arrows in green show the corresponding distribution of surface currents. (b) The SST anomaly for the 1982-83 winter. The arrows indicate the corresponding surface current anomaly. (c) The precipitation and surface wind anomalies (arrows) for the 1982-83 winter.

Fig.3: A schematic showing the role of Tw-Tc in the coupled tropical ocean-atmosphere system.

Fig.4: Time-mean equatorial upper ocean temperature response to an enhanced tropical heating for the case without ENSO (a) and the case with ENSO (b). Shown are the results from experiments of Pair II listed in Table 1. Data used for the calculations here are the same as used for obtaining changes in Tw and Tc in Table 1. The thin dashed contours indicate the mean isentropes of the control run.

Fig. 5: Response of ENSO in the coupled model to an increase in the tropical heating. Shown are time series of Niño3 SST from a control run (solid line) and a perturbed run (dashed line).

Fig.6: Differences in the equatorial upper ocean temperature between the perturbed run and the control run during the La Niña phase (a) and during the El Niño phase (b). The results are from pair II (see legends of Table 1). The 6 cycles of the last 23-years of a 27-year-long run are used in this calculation.

Fig.7: A schematic showing the “ocean tunnel” and how a cooling from the subtropical surface may destabilize the equatorial Pacific ocean-atmosphere system.

Fig.8: Time-mean equatorial upper ocean temperature response to an enhanced subtropical cooling for the case without ENSO (a) and the case with ENSO (b). Anomalous subtropical cooling—a reduction in SSTp—starts at 10^{o} S(N) for this case and increases monotonically with latitude to a fixed value 1^{o}C at 30^{o}S(N). The last 3 years of data of a 27-yr-long run are used in the calculation for the case without ENSO. For the case with ENSO, the last 23 years of a 40-year long run are used. Not like the almost instantaneous response of ENSO to an increase in the tropical heating, there is a delay for the onset of the regime with stronger ENSO in response to an increase in subtropical cooling. Consequently there is a need for a longer run to obtain a time series of Niño3 SST that is representative of the regime.

Figure 9: (a) Response of ENSO in the coupled model to an increase in the subtropical cooling. Shown are time series of Niño3 SST from a control run (solid line) and a perturbed run (dashed line).

Figure 10: Differences in the equatorial upper ocean temperature between the perturbed run and the control run during the La Niña phase (a) and during the El Niño phase (b). The results are from pair II (see legends of Table II). The 6 cycles of the last 23-years of a 27-year-long run are used in this calculation.

Figure 11: Same as Figure 8 except for a meridional section for the central Pacific (160 ^{o}E -210^{o}E). (a) Response without ENSO; (b) Response with ENSO.

Figure 12: A schematic showing the difference between the revised paradigm and the traditional paradigm.

Table I

perturbation type	experiment type	change of Tw (°c)	change of Tc (°c)	change of Tw-Tc (°c)
Pair I (5°S-5°N)	No ENSO	1.03	0.0050	1.02
	With ENSO	0.81	0.76	0.053
Pair II (10°S-10°N)	No ENSO	1.38	0.036	1.34
	With ENSO	0.97	0.83	0.14
Pair III (15°S-15°N)	No ENSO	0.95	0.24	0.71
	With ENSO	0.55	0.63	-0.085

Table II

perturbation type	experiment type	change of Tw (°c)	change of Tc (°c)	change of Tw-Tc (°c)
Pair I 30°N(S)-5°N(S)	No ENSO	-0.13	-0.75	0.62
	With ENSO	-0.67	-0.45	-0.22
Pair II 30°N(S)-10°N(S)	No ENSO	-0.10	-0.63	0.53
	With ENSO	-0.49	-0.23	-0.26
Pair III 30°N(S)-15°N(S)	No ENSO	-0.060	-0.67	0.61
	With ENSO	-0.62	-0.25	-0.37

Fig. 1

(a)

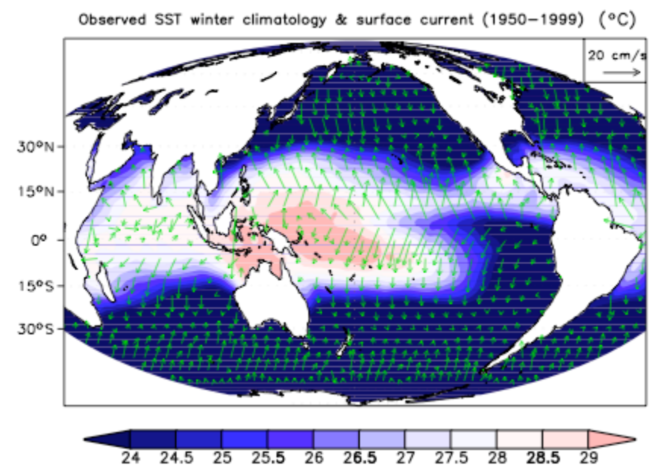
Observed SST winter climatology & surface current (1950–1999) (°C)
20 cm/s
30°N
15°N
0°
15°S
30°S
24 24.5 25 25.5 26 26.5 27 27.5 28 28.5 29

(b)

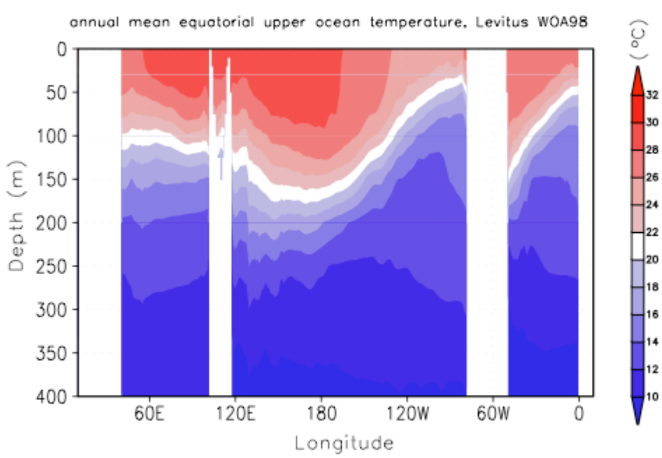
annual mean equatorial upper ocean temperature, Levitus WOA98
Depth (m)
0
50
100
150
200
250
300
350
400
60E 120E 180 120W 60W 0
Longitude
(°C)
32 30 28 26 24 22 20 18 16 14 12 10

(c)

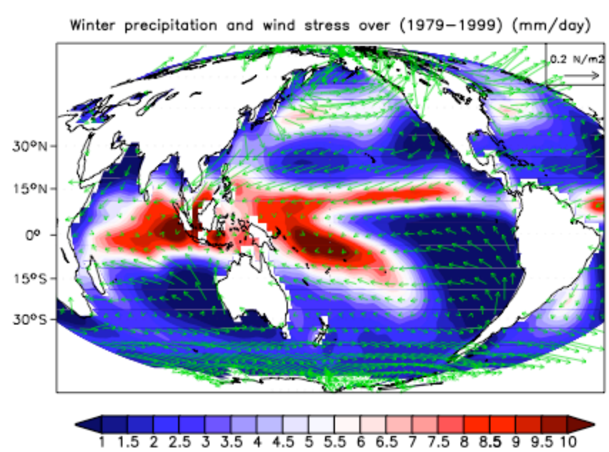
Winter precipitation and wind stress over (1979–1999) (mm/day)
0.2 N/m2
30°N
15°N
0°
15°S
30°S
1 1.5 2 2.5 3 3.5 4 4.5 5 5.5 6 6.5 7 7.5 8 8.5 9 9.5 10

Fig.2

(a)

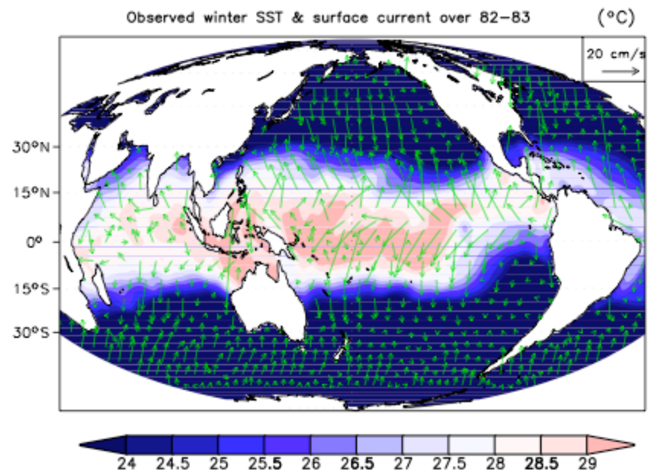
Observed winter SST & surface current over 82–83
(°C)
20 cm/s
30°N
15°N
0°
15°S
30°S
24 24.5 25 25.5 26 26.5 27 27.5 28 28.5 29

(b)

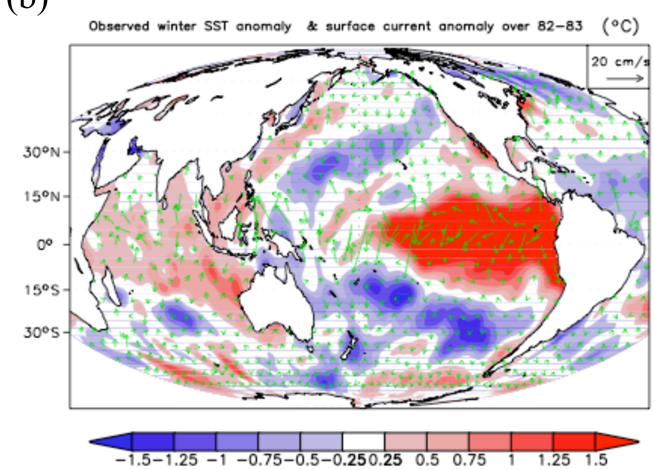
Observed winter SST anomaly & surface current anomaly over 82–83
(°C)
20 cm/s
30°N
15°N
0°
15°S
30°S
−1.5 −1.25 −1 −0.75 −0.5 −0.25 0.25 0.5 0.75 1 1.25 1.5

(c)

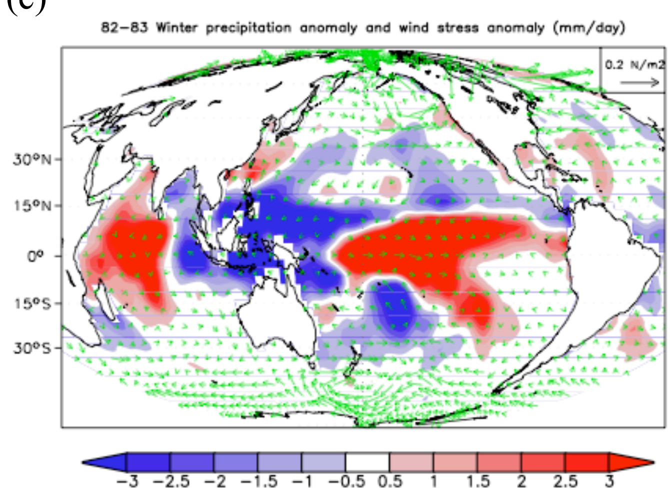
82–83 Winter precipitation anomaly and wind stress anomaly (mm/day)
0.2 N/m2
30°N
15°N
0°
15°S
30°S
−3 −2.5 −2 −1.5 −1 −0.5 0.5 1 1.5 2 2.5 3

Fig.3

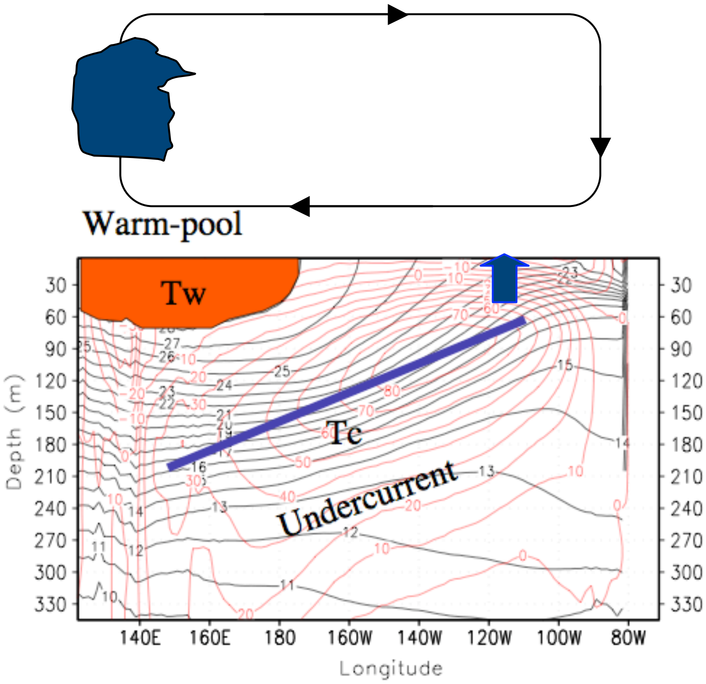
Warm-pool
Tw
Tc
Undercurrent
Depth (m)
Longitude
140E
160E
180
160W
140W
120W
100W
80W
30
60
90
120
150
180
210
240
270
300
330

Fig.4

(a)

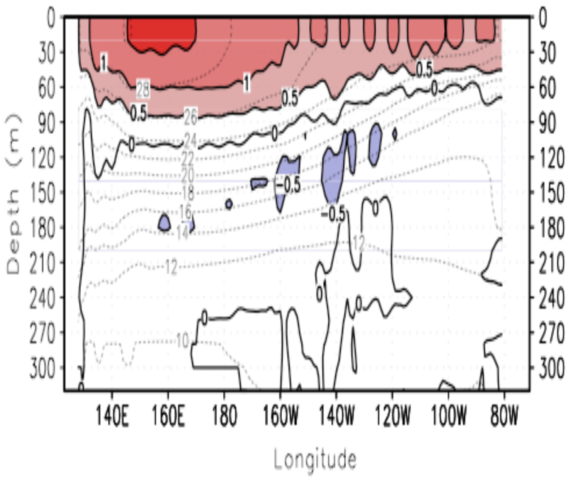
Depth (m)
Longitude
140E 160E 180 160W 140W 120W 100W 80W
0 30 60 90 120 150 180 210 240 270 300

(b)

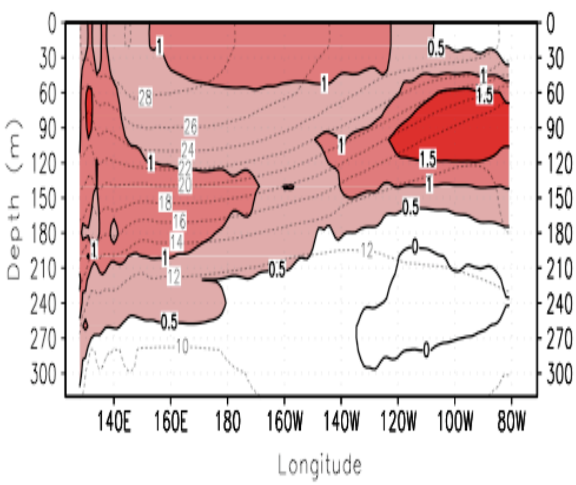
Depth (m)
Longitude
140E 160E 180 160W 140W 120W 100W 80W
0 30 60 90 120 150 180 210 240 270 300

Fig. 5

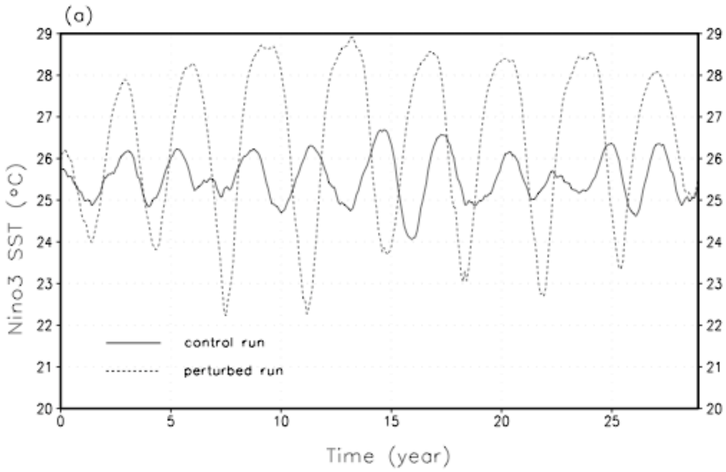

Fig. 6

(a)

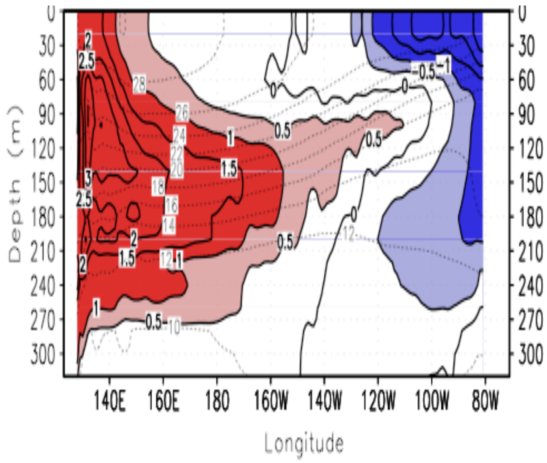
Depth (m)
Longitude
140E 160E 180 160W 140W 120W 100W 80W

(b)

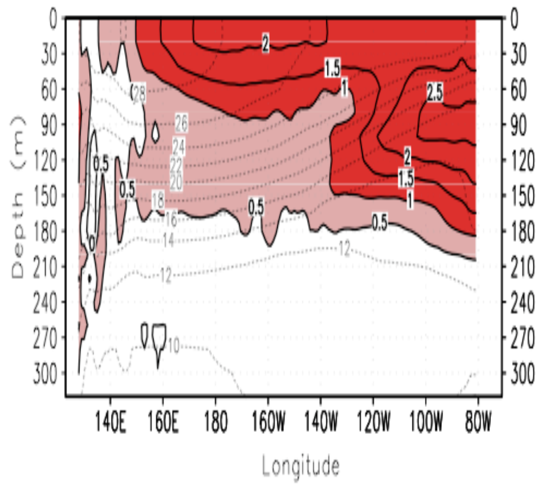
Depth (m)
Longitude
140E 160E 180 160W 140W 120W 100W 80W

Fig. 7

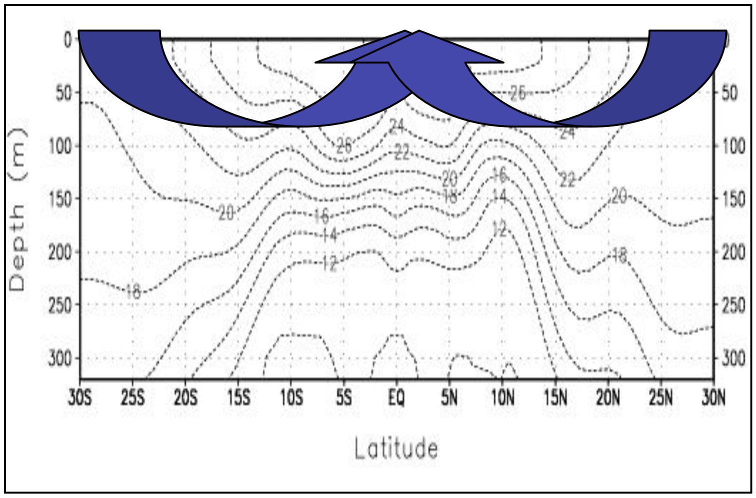
Depth (m)
Latitude
0
50
100
150
200
250
300
30S
25S
20S
15S
10S
5S
EQ
5N
10N
15N
20N
25N
30N
26
24
22
20
18
16
14
12

Fig. 8

(a)

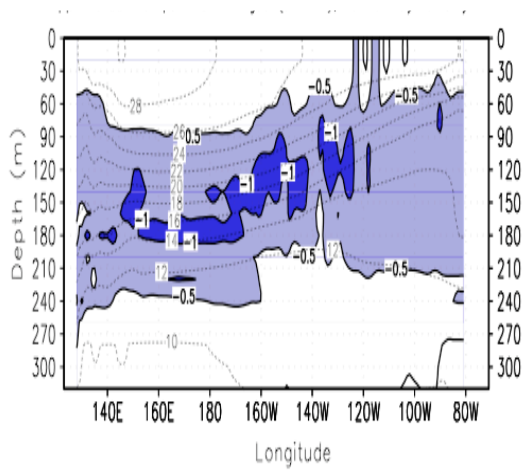
Depth (m)
0
30
60
90
120
150
180
210
240
270
300
140E
160E
180
160W
140W
120W
100W
80W
Longitude

(b)

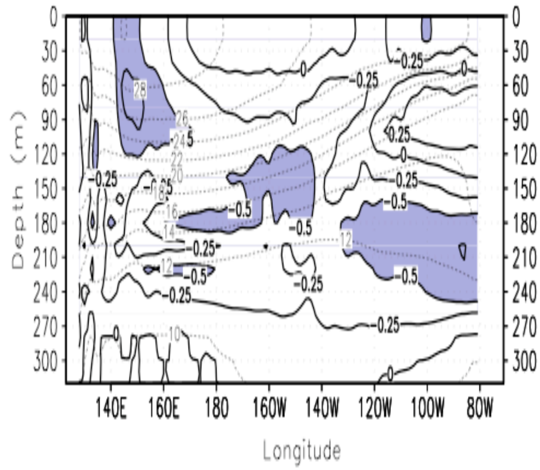
Depth (m)
0
30
60
90
120
150
180
210
240
270
300
140E
160E
180
160W
140W
120W
100W
80W
Longitude

Fig. 9

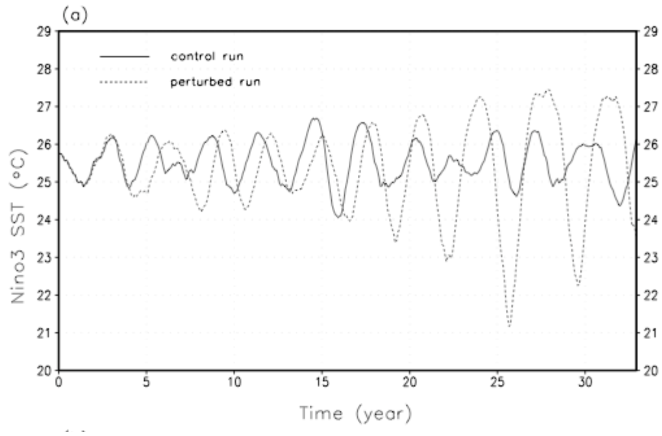

Fig. 10

(a)

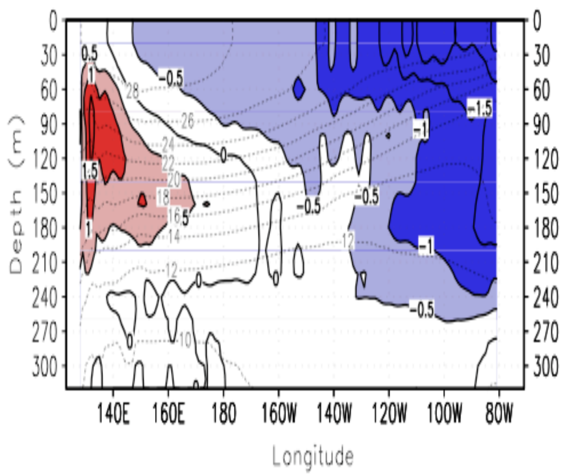
Depth (m)
Longitude
140E 160E 180 160W 140W 120W 100W 80W
0 30 60 90 120 150 180 210 240 270 300

(b)

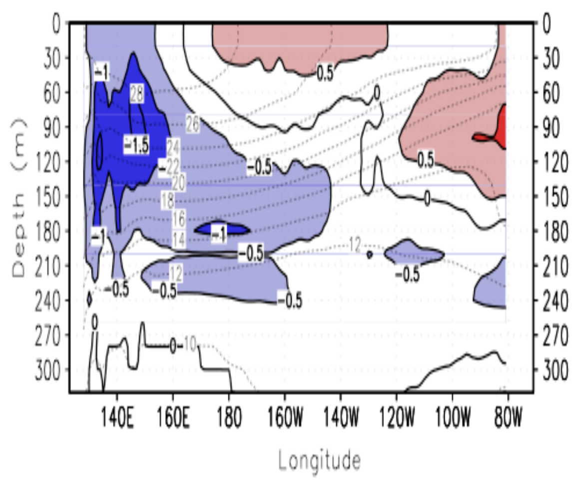
Depth (m)
Longitude
140E 160E 180 160W 140W 120W 100W 80W
0 30 60 90 120 150 180 210 240 270 300

Fig. 11

(a)

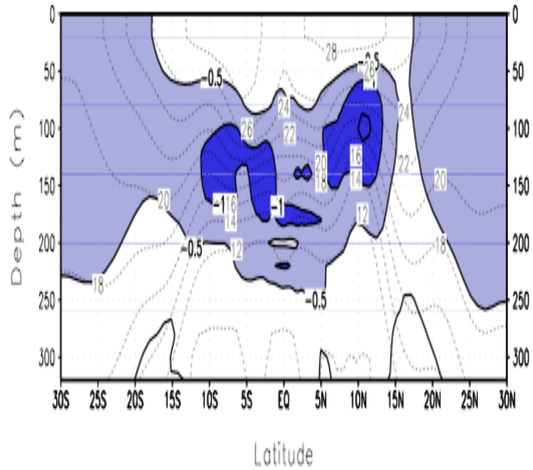
Depth (m)
Latitude
30S 25S 20S 15S 10S 5S EQ 5N 10N 15N 20N 25N 30N
-0.5
-1

(b)

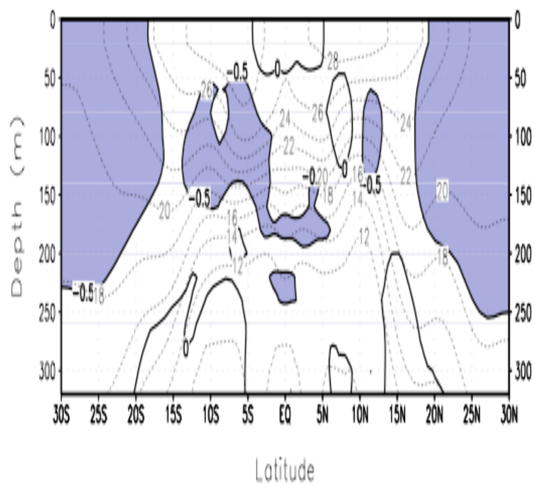
Depth (m)
Latitude
30S 25S 20S 15S 10S 5S EQ 5N 10N 15N 20N 25N 30N
-0.5
0

Fig. 12

Existing Paradigm:

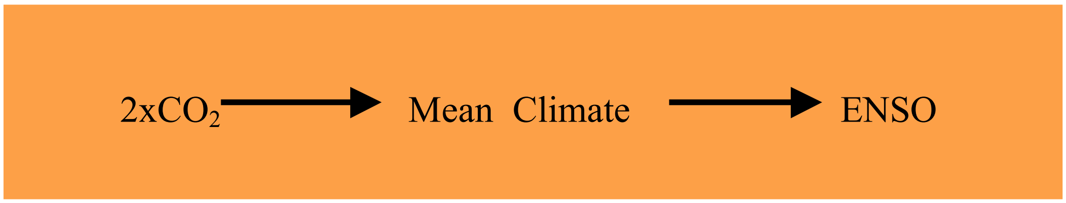

A Revised Paradigm: